SEAWAT 2000: modelling unstable flow and sensitivity to discretization levels and numerical schemes

A. Al-Maktoumi · D. A. Lockington · R. E. Volker

Abstract A systematic analysis shows how results from the finite difference code SEAWAT are sensitive to choice of grid dimension, time step, and numerical scheme for unstable flow problems. Guidelines to assist in selecting appropriate combinations of these factors are suggested. While the SEAWAT code has been tested for a wide range of problems, the sensitivity of results to spatial and temporal discretization levels and numerical schemes has not been studied in detail for unstable flow problems. Here, the Elder-Voss-Souza benchmark problem has been used to systematically explore the sensitivity of SEAWAT output to spatio-temporal resolution and numerical solver choice. A grid size of 0.38 and 0.60% of the total domain length and depth respectively is found to be fine enough to deliver results with acceptable accuracy for most of the numerical schemes when Courant number (Cr) is 0.1. All numerical solvers produced similar results for extremely fine meshes; however, some schemes converged faster than others. For instance, the 3rd-order total variation-diminishing method (TVD3) scheme converged at a much coarser mesh than the standard finite difference methods (SFDM) upstream weighting (UW) scheme. The sensitivity of the results to Cr number depends on the numerical scheme as expected.

Résumé Une analyse systématique montre la sensibilité des résultats obtenus avec le code SEAWAT aux différences finies en fonction du choix du dimensionnement du maillage, du pas de temps et du schéma numérique dans des problèmes d'écoulement instable. Des règles générales aidant à la sélection de combinaisons appropriées pour ces facteurs sont proposées. Si le code SEAWAT a été testé pour une large gamme de problèmes, la sensibilité des résultats aux différents niveaux de discrétisation spatiale et temporelle et aux schémas numériques n'a pas été étudiée en détail pour les problèmes d'écoulement instable. Ici, le problème de référence de Elder-Voss-Souza a été utilisée pour étudier systématiquement la sensibilité des résultats de SEAWAT en fonction du choix de la résolution spatio-temporelle et du solveur numérique. Une taille de maillage de respectivement 0.38 et 0.60% de la longueur et de la profondeur du domaine total, s'est montrée être suffisamment fine pour produire des résultats avec des précisions acceptables pour la plupart des schémas numériques pour un nombre de Courant (Cr) de 0.1. Tous les solveurs numériques ont produit des résultats similaires pour des mailles extrêmement petites, cependant, certains schémas ont convergé plus rapidement que d'autres. Par exemple, le schéma à variation totale décroissante d'ordre 3 (TVD3) a convergé pour un maillage beaucoup plus grossier que le schéma des méthodes standards de différences finies (SFDM) avec pondération amont (UW en anglais). La sensibilité des résultats au nombre de Cr dépend comme prévu du schéma numérique.

Resumen Un análisis sistemático muestra como los resultados del código de diferencia finita SEAWAT son sensibles a la selección de la dimensión de la malla, el intervalo de tiempo, y el esquema numérico para problemas de flujo inestable. Se sugieren lineamientos para asistir en la selección de combinaciones apropiadas de estos factores. Mientras que el código SEAWAT se ha probado para un amplio rango de problemas, no se han estudiado en detalle la sensibilidad de resultados a los niveles de discretización temporal y espacial y los esquemas numéricos para problemas de flujo inestable. Aquí se ha usado el problema de análisis comparativo Elder-Voss-Souza para explorar sistemáticamente la sensibilidad de la salida de SEAWAT con la selección de la solución numérica y la resolución temporal y espacial. Un tamaño de malla del 0.38 y 0.6% de la profundidad y longitud del entorno total, respectivamente, se encontró que era suficientemente fina para aportar resultados con precisión aceptable para la mayoría de esquemas numéricos cuando el número de Courant (Cr) es 0.1. Todas las soluciones numéricas generaron resultados similares para mallas extremadamente finas; sin embargo, algunos

Received: 26 December 2005 / Accepted: 24 January 2007
Published online: 20 February 2007

Electronic supplementary material The online version of this article (doi:10.1007/s1004000701642) contains supplementary material, which is available to authorized users.

A. Al-Maktoumi (✉) · D. A. Lockington · R. E. Volker
Centre for Water Studies, School of Engineering,
The University of Queensland,
Brisbane, 4072, Australia
e-mail: s4051052@student.uq.edu.au
Tel.: +61-7-33653508
Fax: +61-7-33654599

 DOI 10.1007/s10040-007-0164-2

esquemas convergieron más rápido que otros. Por ejemplo, el esquema del Método de Disminución de Variación de Orden Total (TVD3) convergió en una malla mucho más gruesa que la del esquema de Pesado Aguas Arriba (UW) de los Métodos de Diferencia Finita Standard (SFDM). Tal y como se esperaba la sensibilidad de los resultados del número Cr dependen del esquema numérico.

Keywords Grid sensitivity · Numerical modeling · Unstable flow · Convection · SEAWAT

Introduction

The finite-difference, variable density groundwater code SEAWAT has been validated and tested for various benchmark problems (e.g., Guo and Langevin 2002; Langevin et al. 2003; Bakker et al. 2004; Langevin and Guo 2006); however, a systematic and detailed study of its sensitivity to spatial and temporal discretizations has not yet been undertaken for unstable flow problems (note that recently Zimmermann et al. (2005) presented a sensitivity analysis for SEAWAT and other codes for an unstable flow problem associated with evapoconcentration of salts on islands). For unstable problems, the results of different codes (e.g., FEFLOW, SUTRA, ROCKFLOW, and 2DFEMFAT) are found to be sensitive to the level of spatial and temporal discretizations and to the numerical algorithm used to approximate the solution of the transport equation (Voss and Souza 1987; Schincariol et al. 1994; Ibaraki 1998; Diersch and Kolditz 1998; Zhang 2000; Woods et al. 2003).

A well-studied unstable solute transport problem was published by Voss and Souza (1987); it was based on the heat convection problem of Elder (1967) and referred to as EVS in what follows. The unstable EVS problem is particularly sensitive to choices in discretization and solvers with a major feature being the resulting variation in the direction of the flow and transport at the centre of the domain (up/down welling) (Diersch and Kolditz 1998, 2002; Zhang 2000; Woods et al. 2003). For instance, Oldenburg and Pruess (1995) showed that for a fine mesh (i.e., the EVS domain is discretized with a regular mesh of around 5,000 cells: resolution level R2 in Table 1) there is an up-flow at the centre of the domain. This result is similar to that of Elder's original experimental results (Elder 1967) and has been obtained by, for example, Kolditz et al. (1998), Holzbecher (1998), Ackerer et al. (1999), Prasad (2000), and Oltean and Bues (2001). Using finer grids (R3; Table 1), Frolkovic and Schepper (2000) show a small central down-welling. The central down-welling is also observed with coarse meshes (i.e., R1; Table 1) in Voss and Souza (1987), Oldenburg and Pruess (1995), Kolditz et al. (1998), and Mazzia et al. (2001). It has been noted that the solution is very sensitive to perturbations such that it is difficult to be confident about which are the correct results (Frolkovic and Schepper 2000; Woods et al. 2003). Since the central up-flow pattern matches the Elders laboratory observations, and others (e.g., Kolditz et al. 1998; Holzbecher 1998; Ackerer et al. 1999; Prasad 2000; Oltean and Bues 2001) have confirmed these results, it will be considered here to be the physically correct case and referred to as such in what follows.

Temporal discretizations are also found to affect the salinity patterns and flow field (Diersch and Kolditz 1998). Diersch and Kolditz (1998) demonstrated that satisfying the standard stability criteria of the Peclet (Pe) and Courant (Cr) numbers does not guarantee good convergence for the EVS problem.

Given the increasing popularity of SEAWAT, it is appropriate to systematically explore the code's sensitivity to spatio-temporal discretization, and choice of numerical transport solvers, for unstable dynamics as represented by the classic EVS problem. In this study, various mesh sizes have been used (up to 82,000 cells) with different numerical schemes and temporal discretizations to explore the sensitivity of the predicted solute concentration fields. This will provide an approximate guide for SEAWAT users in their selection of grid and time step sizes (for a given solver) for modelling problems, which feature unstable flows. The results will be expressed using both qualitative and quantitative measures.

SEAWAT summary

SEAWAT couples the flow and transport equations of two widely accepted codes (MODFLOW (McDonald and Harbaugh 1988; Harbaugh et al. 2000) and MT3DMS (Zheng and Wang 1999)) with some modifications to include density effects based on the extended Boussinesq

Table 1 Spatial resolution levels used in the study (standard Elder-Voss-Souza problem)

Resolution level	Resolution class	Grid size (dz, dx) m	No. of layers × columns	Resolution (No. of cells)
R1	Coarse	5.556×13.636	27×44	1,118
R2	Fine	2.769×6.818	53×88	4,664
R3	Very fine	1.361×3.409	105×176	18,480
R4	Extremely fine	0.917×2.273	157×264	41,448
R5	Extremely fine	0.791×1.364	183×440	80,520

 DOI 10.1007/s10040-007-0164-2

assumption. It reads and writes standard MODFLOW and MT3DMS input and output files so that most existing pre- and post-processors for those packages can be used. The governing flow equation in SEAWAT is (after Guo and Langevin 2002):

$$\frac{\partial}{\partial x_i}\left[\rho K_{fx}\left(\frac{\partial_{hf}}{\partial x_i}+\frac{\rho-\rho_f}{\rho_f}\frac{\partial L}{\partial x_i}\right)\right] + \frac{\partial}{\partial y_j}\left[\rho K_{fy}\left(\frac{\partial K_{fy}}{\partial y_j}+\frac{\rho-\rho_f}{\rho_f}\frac{\partial L}{\partial y_i}\right)\right] + \frac{\partial}{\partial z_k}\left[\rho K_{fz}\left(\frac{\partial h_f}{\partial z_k}+\frac{\rho-\rho_f}{\rho_f}\frac{\partial L}{\partial z_k}\right)\right] = \rho S_f\frac{\partial h_f}{\partial t}+\theta\frac{\partial \rho}{\partial C}\frac{\partial C}{\partial t}-\rho_s q_s \quad (1)$$

where x, y, z are coordinate axis, i, j, k are column, row, and layer indices respectively; K_f is equivalent freshwater hydraulic conductivity (L T^{-1}); S_f is equivalent freshwater specific storage (L^{-1}); h_f is equivalent freshwater head (m); t is time (T); θ is effective porosity (dimensionless); C is solute concentration (M L^{-3}); ρ_s is fluid density of source or sink water (M L^{-3}); L is the cell centre elevation (L); and q_s is the volumetric flow rate of sources and sinks per unit volume of aquifer (T^{-1}). The transport equation is:

$$\frac{\partial(\theta C^k)}{\partial t}=\frac{\partial}{\partial_{X_i}}\left(\theta D_{ij}\frac{\partial_C^k}{\partial_{X_j}}\right)-\frac{\partial}{\partial_{X_i}}\left(\theta v_i c^k\right)+q_s C_s^k + \sum R_n \quad (2)$$

where c^κ is dissolved concentration of species κ (M L^{-3}); D_{ij} is the hydrodynamic dispersion tensor (L^2 T^{-1}); v_i is linear pore water velocity (L T^{-1}); C_s^k is concentration of the source or sink flux for species κ (M L^{-3}); and ΣR_n is the chemical reaction term (M L^{-3} T^{-1}).

For details about the derivation and modification of the governing equations, readers are directed to the SEAWAT manual (Guo and Langevin 2002). A number of numerical schemes are available for solving the flow and transport equations. For the flow equation, the default preconditioned conjugate gradient package 2 (PCG2) solver is used for all the simulations in this study. The convergence criterion is set to 1×10^{-7} m for the head change. The numerical solvers of the transport equation that will be explored in this paper are the standard finite difference methods (SFDM), e.g., upstream weighting (UW), and central in space (CIS); mixed Eulerian-Lagrangian methods (MELM), e.g., method of characteristics (MOC), modified method of characteristics (MMOC), and hybrid method of characteristics (HMOC); and the 3rd-rrder total variation-diminishing method (TVD3). SEAWAT 2000 contains explicit and implicit iterative options for solving Eqs. (1) and (2) (Guo and Langevin 2002; Langevin et al. 2003). For the implicit option, Eqs. (1) and (2) are solved simultaneously through a Picard iterative strategy for each transport step; SEAWAT 2000 uses double precision throughout so that round-off error is assumed to be negligibly small.

Methodology

Elder-Voss-Souza problem setup and spatial resolution

Figure 1 depicts the setup of the standard Elder-Voss-Souza problem with resolution level (R1) as detailed in Table 1. The boundary conditions are as follows. For the flow equation, zero constant hydraulic head is imposed at the two upper corners of the domain and no flux on all other boundaries. For the mass transport equation, zero concentration is set along the base and C=287.5 kg/m^3 is imposed at the source. On the remaining boundaries, zero dispersive flux is enforced. Zero value of concentration is used for the initial solute distribution. Other parameters are presented in Table 2.

The mesh size will be refined successively to four finer resolutions as shown in Table 1 and Fig. 2.In all cases, the dimensions of the source are kept constant (see Woods et al. 2003). Figure 2 presents the grid sizes of the R1–R5 as a percentage of the total horizontal length (dx) and depth (dz) of the flow domain.

Stability criteria

Stability is usually characterized in terms of dimensionless parameters such as the Rayleigh number (Ra), wavelength of perturbation (λ), Nusselt number (Nu), and Peclet number (Pe) (Wooding 1969; Schincariol et al. 1994, 1997; Diersch and Kolditz 1998; Simmons and Narayan 1997; Woods et al. 2003; Weatherill et al. 2004, among others). Ra in this study is calculated to be ≈400. Nu is calculated to be 41.6. Theoretically a stable system should

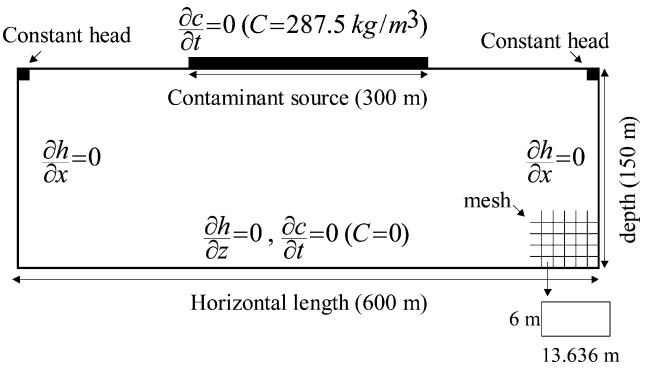

Fig. 1 Sketch of Elder-Voss-Souza (EVS) benchmark problem with resolution level of R1

DOI 10.1007/s10040-007-0164-2

Table 2 Other parameters for the Elder-Voss-Souza problem

Parameter	Value	Dimension
Porosity	0.1	–
Hydraulic conductivity (H and V)[a]	0.411	m/day
Longitudinal and transversal dispersivity	0	m
Molecular dispersivity	0.308	m^2/day
Density of freshwater	1,000	kg/m^3
Density of solute	1,200	kg/m^3
Concentration at the source (C)	287.5	kg/m^3
Courant number (Cr)	0.1	–
Convergence criteria (γ)	1×10^{-5}	kg/m^3

[a] H and V are horizontal and vertical hydraulic conductivity, respectively

have Nu ~1 as all solute transport is by diffusion (Weatherill et al. 2004). Nu>1 indicates that the system is unstable and the solute transport takes place by convection along with diffusion. The Pe is calculated to be 8.03 (for R1) to 0.82 (for R5; Fig. 3). The equations for these dimensionless criteria are taken from Weatherill et al. (2004).

Temporal discretization

In SEAWAT, the temporal discretization scheme is a combination of that used in MODFLOW and MT3DMS. SEAWAT divides the stress periods into time steps. These time steps are further divided into transport steps by the program based on stability criteria of Zheng and Wang (1999). SEAWAT solves Eqs. (1) and (2) for each transport time step using explicit or implicit approaches (see Langevin et al. 2003). For all the runs in this study, Eqs. (1) and (2) are solved implicitly using the generalized conjugate gradient (GCG) solver. Guo and Langevin (2002) explain both of these options in detail.

The time step (TS) length in SEAWAT is set by choosing the value of Cr, where

$$C_r = \frac{v\Delta t}{\Delta \ell} \tag{3}$$

where v (L T^{-1}) is the velocity, Δt (T) is the time step, and $\Delta \ell$ (L) is grid size in the direction of v.

While time stepping is adaptive, the effect of the TS size on the evolution of the salinity distribution is explored by setting different values of Cr in the transport solver. The numerical schemes considered are: SFDM (UW), SFDM (CIS), MMOC, and TVD3. Not all of the numerical schemes were used. From the MELM group, MMOC is selected due to its computational efficiency. The grid resolution R4 is selected for all runs to limit the variation in the results to the effect of temporal discretization. Table 3 presents the numerical simulations to be used.The range of Cr selected is based on the Diersch and Kolditz (1998) study using FEFLOW. They found that Cr 1 is not enough to ensure good convergence.

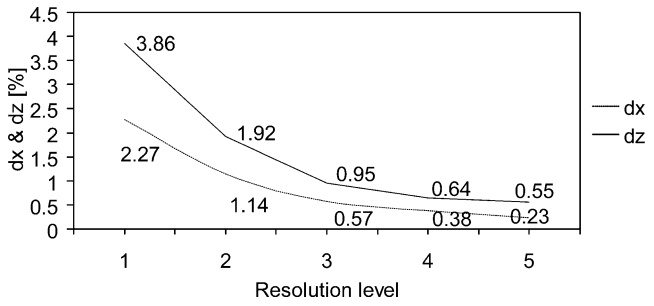

Fig. 2 Grid cell dimensions (dx and dz) used for each resolution level shown as a percentage of the total length and depth of the flow domain

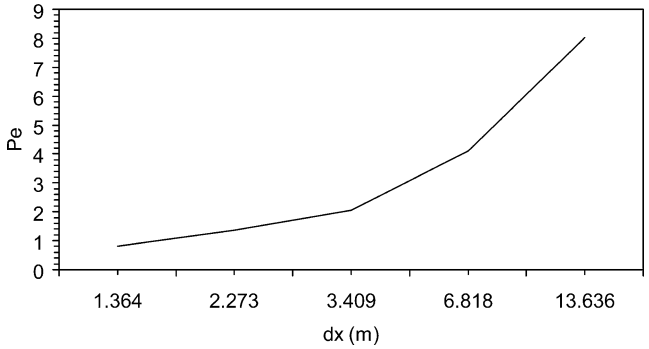

Fig. 3 Peclet number (Pe) as a function of grid dimension dx

The effect of choice of numerical transport schemes/solvers

Given that MT3DMS allows the use of different numerical schemes to solve the advection term of the transport equation. The effect of choice of numerical scheme on results will be studied for different grid resolution levels and Cr numbers as defined above in Tables 1 and 3.

Measures for comparison

Density dependent flow simulators are commonly tested qualitatively by comparing the code outputs (mainly isochlors, which is salinity level in what follows) for a well-known benchmark (e.g., EVS problem) with code outputs from other codes. This qualitative comparison

Table 3 The numerical simulations for the temporal discretization study

Run No.	Cr number	Resolution level	Numerical scheme
1	1	R4	SFDM(UW), SFDM(CIS), MMOC, TVD3
2	0.75	R4	SFDM(UW), SFDM(CIS), MMOC, TVD3
3	0.5	R4	SFDM(UW), SFDM(CIS), MMOC, TVD3
4	0.1	R4	SFDM(UW), SFDM(CIS), MMOC, TVD3

 DOI 10.1007/s10040-007-0164-2

may not allow easy detection of discrepancies (Prasad and Simmons 2004) and so does not necessarily ensure that the model is adequately tested. Consequently, quantitative criteria such as the maximum depth of penetration (MDP) and the total mass of contaminant (Mt) were also considered for comparison purposes (see Prasad and Simmons 2004).

The MDP is a useful quantitative indicator because it gives information about the maximum depth impacted by a predefined solute concentration in a unit time. The MDP will be calculated for a selected isochlor (C=0.5) for each run. The Mt indicator corresponds to the total mass load at a selected depth across the horizontal dimension of the domain at a specified simulation time. In this study, Mt for a horizontal slice of 5.5 m thickness, the top of which is located at 60.5 m below the source, will be calculated after 10 years for use in comparisons.

Results and discussion

Spatial resolution effects

Qualitative analysis

Results are presented illustrating the differences between convection patterns for the five resolution levels and choice of numerical transport schemes, in Fig. 4 and as on-line electronic supplementary material ESM(1). Figure 4 presents the 0.2 (57.5 kg/m^3) and 0.6 (172.5 kg/m^3) isochlors at 7 and 20 years respectively for SFDM (UW), MMOC, and TVD3 schemes (results for the other schemes and for more time intervals are available on-line (ESM 1)). Results for the first three resolutions show significantly different convection patterns (isochlor shape) between the numerical schemes.

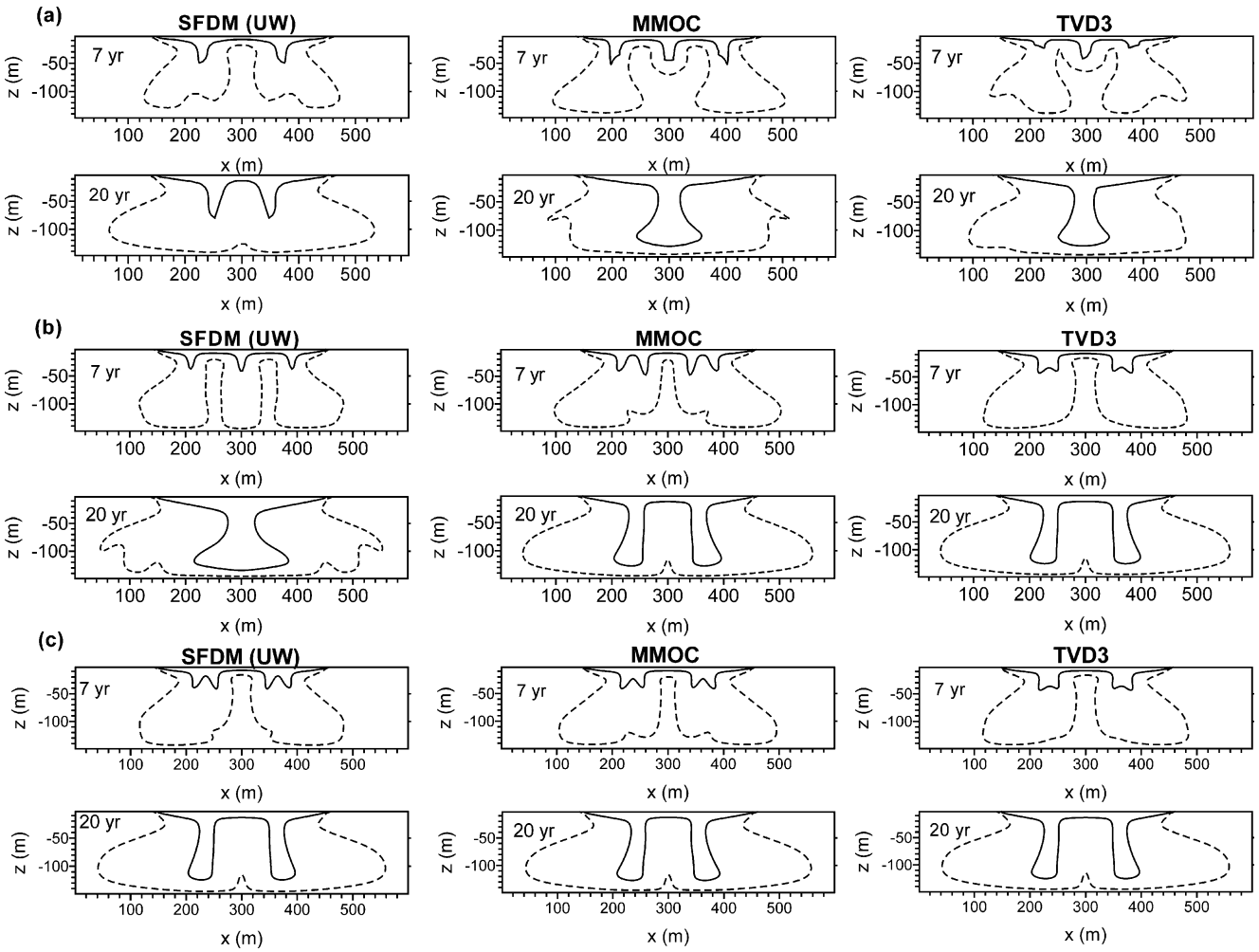

Fig. 4 The 0.2 (*dashed line*) and 0.6 (*solid line*) isochlors for the Elder-Voss-Souza problem at time of 7 and 20 years for resolution levels of **a** R1, **b** R3, and **c** R5, and *SFDM (UW)*, *MMOC*, and *TVD3* numerical schemes, using SEAWAT-2000. *z* = depth of the domain, *x* = length of the domain

 DOI 10.1007/s10040-007-0164-2

During the simulation, the number and shapes of evolving dense fingers change due to splitting and fusion processes. Using grid R1, the SFDM (CIS), MMOC, and TVD3 schemes generate down-welling at the centre of the domain which agrees with results from Voss and Souza (1987), Oldenburg and Pruess (1995), and to some extent Elder (1967) for an approximately similar coarse mesh size (R1), whereas the other schemes show an up-welling (see ESM 1) which agrees with Zhang (2000). Zhang (2000) found that the 2DFEMFAT code produces up-welling using a coarse mesh (≈R1). SEAWAT at resolution R1 also produces up-welling if MOC, HMOC or SFDM (UW) schemes are used (see Fig. 4 and ESM 1).

The initial definition of the dense plumes is more pronounced in the plots with finer meshes where the authors expect less numerical dispersion. The salinity evolution patterns are different in terms of central up-welling and down-welling for the first three resolution levels and between all numerical schemes. For example, SFDM (UW) shows central up-welling after 7 years for resolution R1 and central down-welling for R2. The Oldenburg and Pruess (1995) results for 3,968 rectangular elements (R2) show an up-welling at the centre. Kolditz et al. (1998) did not find a central up-welling for a coarse mesh but did for the finer resolution of 4,539 cells (R2). When MOC or HMOC schemes are used, SEAWAT produced an up-welling at the centre for R2, whereas other schemes show down-welling.

The isochlors match well at long times for all schemes after refining the mesh from R2 to R3 with a small discrepancy in the finger dimensions; an exception is the SFDM (UW; Fig. 4 and ESM 1). Likewise, using mesh R4 (see ESM 1) results in concentration patterns (i.e., isochlors) are in good agreement for all selected numerical schemes and times, excluding SFDM (UW). Refining the mesh further to R5 delivers results similar to that of R4. Consistency in the results is assumed to be achieved at mesh resolutions R4 and R5 based on the above qualitative comparison, excluding the SFDM (UW), which agrees only at R5. This finding will be checked further using the quantitative indicators below.

The computational time for a run was found to vary from less than 20 min for the coarse mesh (R1) to 23 h for R5 (MMOC and TVD3 schemes) on a Pentium 4 personal computer, 3 GHz processor with 1 GB RAM. While there are a number of codes used to simulate the EVS problem, it is not clear which produces the most accurate results. Different codes require different grid sizes to produce similar results. Figure 5 compares results of SUTRA (Voss and Souza 1987), Elder (1967), and SEAWAT, whereas Fig. 6 compares results from finite difference (SEAWAT) and finite element codes (FEFLOW and ROCKFLOW).

Quantitative analysis

Maximum depth of penetration (MDP) Figure 7 (a) shows the effect of spatial resolution on the MDP (see Methodology section) of the 0.5 isochlor over time for the MMOC solver. In general, use of finer meshes (R3, R4, and R5) results in a maximum penetration depth greater than that for the coarser meshes (R1 and R2). A similar MDP is observed for resolutions R4 and R5. Among the finer meshes (R3 to R5), results for R3 show the highest penetration depth in the first 10 years. However, after 10 years, the MDP curves show similar values for all the finer meshes (R3 to R5). This can be observed also in the contour plots in ESM 1 (for R3). In comparison with finer meshes, the coarser resolutions (R1 and R2) yield a smaller MDP from 5 to 13 years. This is due to the growth of a new finger at the centre such that the growth of the outer fingers is retarded. With time, the outer fingers coalesce with the interior finger causing the steep rise in the MDP curves (due to vertical growth of fingers). The flattening of the MDP curves for the finer meshes (after 15 years) indicates that the steady state is approached as the density contrast decays.

Figure 7b plots the MDP against time for different numerical schemes and grid R3. The curves show there is a difference in the rate of penetration between the different schemes, especially in the period from 2–10 years. In this period, MOC and MMOC (and SFDM (UW) initially) show higher MDP compared with the other schemes (which show relatively similar results to each other). This finding is similar to observations made by Zimmermann et al. (2005) in their recent study of the unstable groundwater flow and salt transport below islands in the Okavango Delta, Botswana. They found that finger development is much faster for the MOC scheme compared to that for TVD3 and SFDM (UW) schemes using SEAWAT and that obtained with their pse2d code. After 10 years, the penetration curves for all methods show good agreement—except for SFDM (UW). After 15 years, the curves level off indicating approach to steady state.

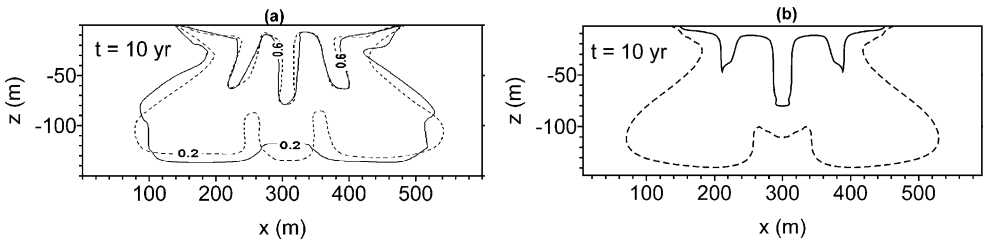

Fig. 5 The 0.2 and 0.6 isochlors at l0 years: **a** Elder (*solid line*), and Voss and Souza *(dashed line*; after Diersch and Kolditz (1998); **b** SEAWAT R1 (1,118 nodes)

 DOI 10.1007/s10040-007-0164-2

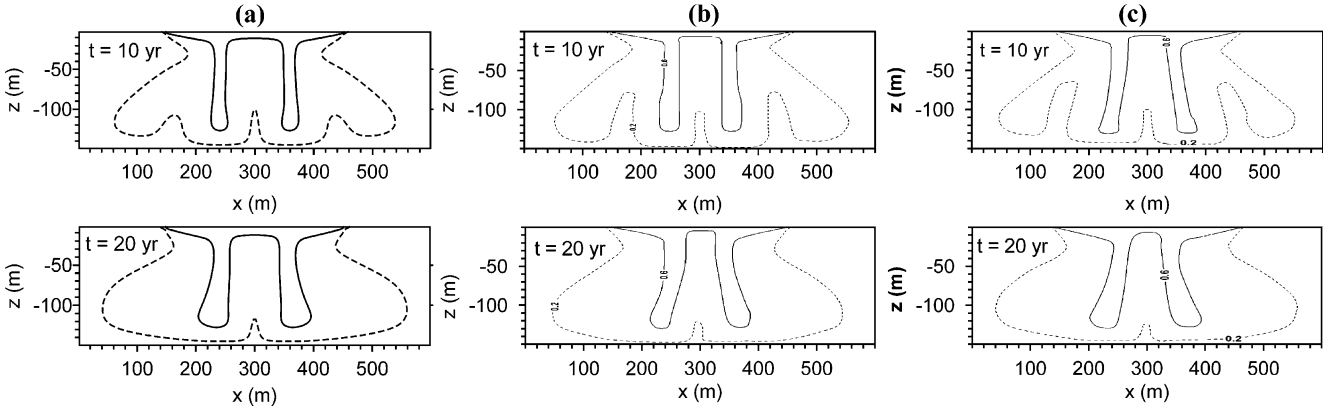

Fig. 6 Comparison of results with those from other codes for 0.2 and 0.6 isochlors for 10, and 20 years. **a** SEAWAT (14,432 nodes). **b** FEFLOW (10,108 nodes). **c** ROCKFLOW (10,108 nodes). **b** and **c** are after Diersch and Kolditz (1998)

Total contaminant mass (Mt) indicator The calculated Mt values are found to vary significantly with grid size and numerical solution scheme. The difference in Mt between schemes is higher for coarser meshes. For example, the difference in Mt between the different numerical schemes is as large as 20% for meshes R1–R3 but can be less than 2% for resolutions R4 and R5; an exception is the result for SFDM (UW). The variation in the Mt curves for meshes R1–R3 reflects the variation of the central up/down welling flow, which was also evident in the qualitative plots.

The value of Mt for the MMOC is found to be larger than for the other schemes for all resolution levels. This corresponds with the observed qualitative difference in isochlors found using this scheme with the results from other schemes (i.e., deeper fingers) even at R5.

Figure 8 indicates that for a given scheme different resolutions might give significantly different mass values if the resolution is coarser than that of R4. The difference in mass between the two extremes of R5–R1 is expected to reflect the effect of numerical dispersion (which of course is large for a coarse mesh) along with other errors such as round off error. It is also important to notice that Mt for R4 and R5 with the SFDM (UW) scheme shows an insignificant difference, whereas the qualitative isochlor plots illustrate discrepancies of central up and down wellings.

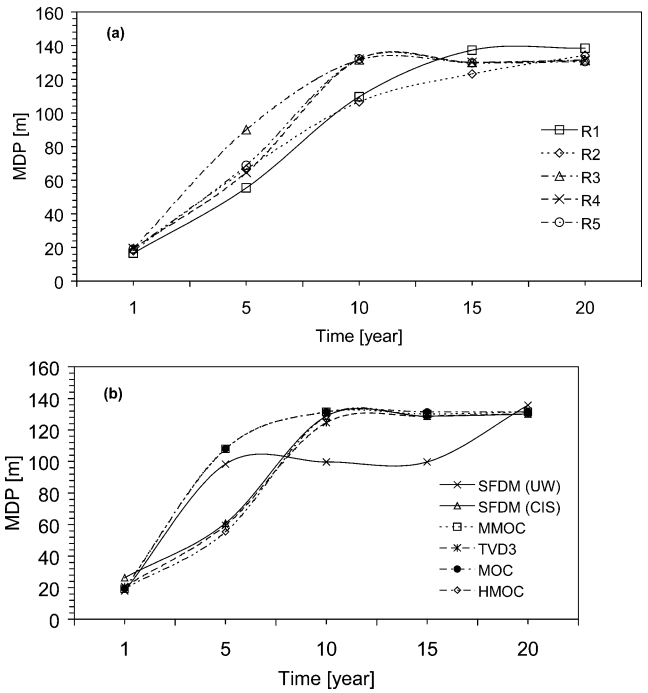

Fig. 7 **a** Maximum depth of penetration (*MDP*) of 0.5 isochlor against time for *MMOC* solver at different resolution levels (*R1–R5*). **b** *MDP* of 0.5 isochlor against time for different numerical schemes using *R3*

Temporal discretization effect

Cr numbers of 0.1, 0.5, 0.75, and 1 are used with the following numerical schemes: SFDM (UW), SFDM (CIS), MMOC, and TVD3. The position of the 0.2 and 0.6 isochlors at different times are compared for different Cr numbers and schemes. Figures 9 and 10 show how the choice of the Cr controls the time step length (TS) and

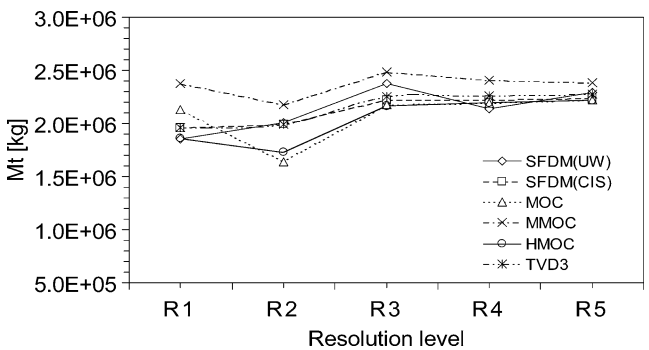

Fig. 8 Total contaminant mass (*Mt*) in the horizontal slice of 5.5 m thickness, the top of which is located at depth 60.5 m below the source, at 10 years for all resolution levels (*R1–R5*) and numerical schemes

 DOI 10.1007/s10040-007-0164-2

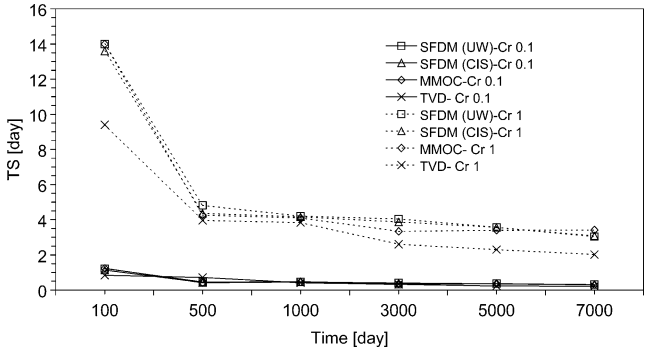

Fig. 9 Variation of time step (*TS*) length with time for different Cr numbers and numerical schemes

the number of inner iterations required for the solution of the transport equation to converge for the different numerical schemes. Results are only presented for Cr 0.1 and 1 for the sake of brevity.

Figure 9 presents variation of the TS length with time. The TS length decreases in the first 500 days of simulation. For example, the decrease for SFDM (CIS) and TVD3 solvers is about 68 and 58% respectively when Cr is 1; and about 63 and 15% when the Cr is 0.1. By the end of the simulation time, the length of TS is reduced by about 90% of the initial value when Cr is reduced by one order of magnitude (1–0.1) for all the numerical schemes. Likewise, the number of inner iterations required to meet convergence criteria is reduced by around 68%.

The higher the Cr (1), the longer is the TS (14 days after 100 days of simulation for MMOC solver) and hence the larger the number of iterations (24) needed for the solution to converge. When Cr is small (0.1), the solution converges within a small number of iterations (7) with a shorter TS of 1.23 days. The number of iterations required for convergence reduces with time (simulation) for the different Cr numbers and solvers. For example, it reduces from 19 iterations at 100 days to 5 iterations at 7,000 days when Cr is 1 and from 5 to 2 iterations when the Cr is 0.1 at the same times for SFDM (CIS) solver.

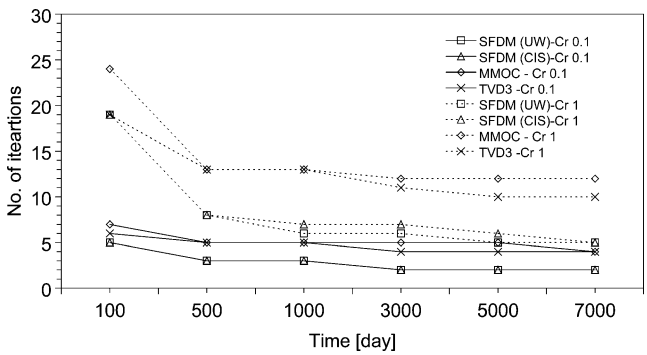

Fig. 10 Change of number of inner iterations with time for the different numerical schemes when *Cr* is 0.1 and 1

Qualitative analysis for temporal discretization

Figure 11 shows the effect of the length of TS on the evolution of salinity distribution at times of 5 and 20 years for SFDM (CIS), MMOC and TVD3 schemes (more results available online in ESM 2). The choice of different Cr numbers produces different convection patterns for a given scheme. Choosing a Cr of 0.1 (for R4) produces similar results for all schemes excluding the SFDM (UW), which produces similar patterns only at R5.Although results for grid size R4 were generally free of artificial oscillations, large Cr numbers (≥0.75) were found to cause oscillations for the SFDM schemes.

Quantitative analysis for temporal discretization

MDP indicator The MDP curves in Fig. 12 show similar trends to those of the spatial resolution study (Fig. 7a). The period in which fingers develop and coalesce is found to be longer (between 3 years and 16 years) for higher Cr (1), whereas it is between 3 years and 10 years for Cr of 0.1. This indicates that the steady state condition is reached faster when the TS is small.

Mt indicator Figure 13 shows the total mass load in the horizontal 5.5 m thick slice that is located at depth of 60.5 m after 10 years of simulation.Figure 13 also shows that the difference between the Mt results using different numerical schemes actually increases with decreasing Cr. A small difference (<2%) between results for the numerical schemes was found at Cr=1, increasing to about 16% for Cr=0.1. Where most schemes (e.g., MMOC and TVD3) show no significant difference in Mt (<2%) over the range of Cr, the SFDM (UW and CIS) schemes are found to be very sensitive to the assigned Cr number (16%). This probably reflects the different schemes' susceptibility to numerical dispersion. In general, Mt is seen to be of limited use as an indicator in this situation.

What numerical scheme to select?

Since different numerical schemes produce different results at different discretization levels, care is required in selecting the numerical scheme and corresponding grid size that will give acceptable results with affordable computational expense. The SFDM (UW) was found to deliver results that only match those of the other schemes at the highest resolution. The other methods produce similar results to each other at coarser spatial resolutions. The SFDM (CIS) suffers from artificial oscillations, which is indicated by negative concentrations, for the first 3 grid sizes and disappears at resolutions R4 and R5. Thus, if the SFDM schemes are to be used, the regular cell dimensions should be ≤0.23% of the total domain length and ≤0.55% of the total depth, and the Cr taken as 0.1. SFDM schemes are found to be the most efficient in terms of computational expense.

 DOI 10.1007/s10040-007-0164-2

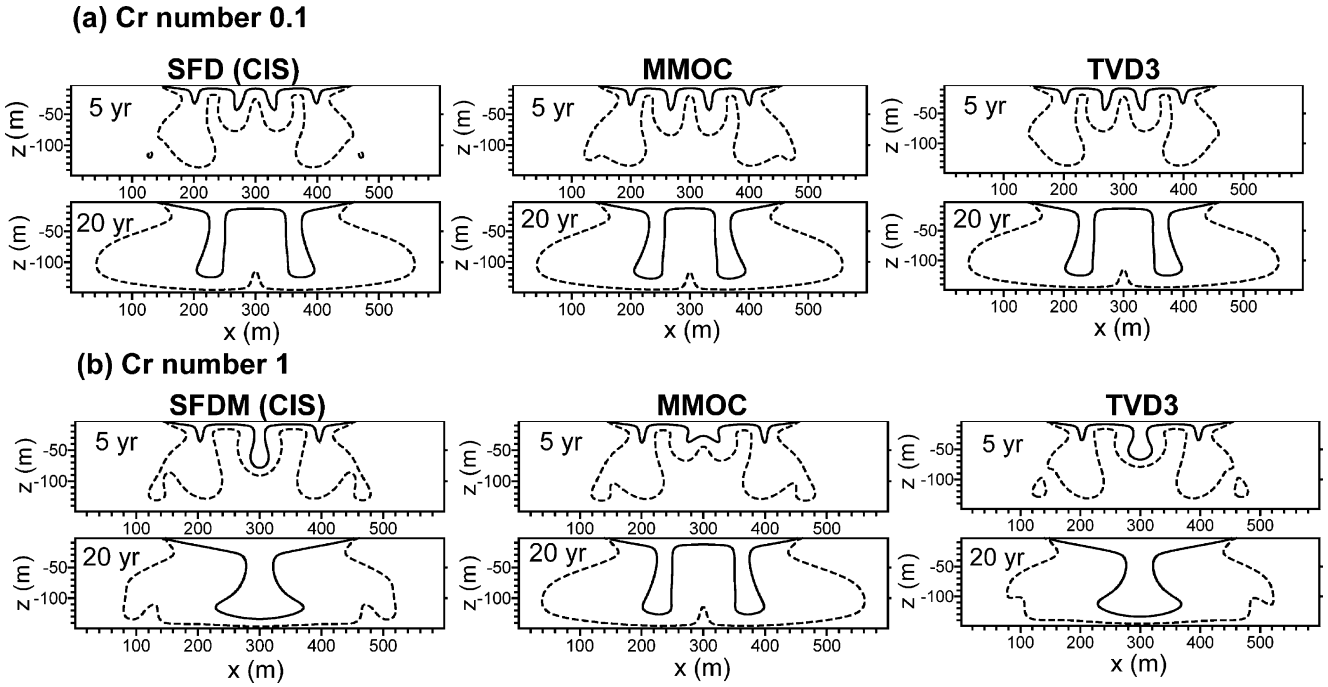

Fig. 11 The 0.2 (*dashed line*) and 0.6 (*solid line*) isochlors for the Elder-Voss-Souza problem at elapsed time intervals of 5, and 20 years for **a** *Cr* number 0.1 and **b** *Cr* number 1, for *SFDM (CIS)*, *MMOC*, and *TVD3* numerical schemes using *R4*

MELMs should be used with caution, especially with the MOC and HMOC schemes. The MELM schemes are expected to lead to a large mass balance discrepancy because they are not entirely based on the principle of mass conservation (Zheng and Bennett 1995). Benson et al. (1998) suggested that using the particle tracking method (MELM) algorithms when modelling highly variable velocity fields requires an extremely fine mesh, as observed in this study. The MOC and HMOC methods were found to be sensitive to input solver parameters such as the maximum number of total moving particles (MAXPART) used in representing the concentration distribution, and other options like the pattern of initial placement (NPLANE), number of particles per cell (NPL and NPH), and minimum and maximum number of particles allowed per cell (NPMIN and NPMAX) (see Chiang and Kinzelbach 1998). Small values for NP cause SEAWAT either to stop or to deliver completely misleading results (i.e., no density driven fingers) (Fig. 14a). When NP is increased the results improve to that of Fig. 14c. It is difficult to tell a priori what the optimal value of NP is, however it can be recommended to start with an NP of more than 100,000 particles, keeping in mind the computational time and the required storage memory. The default NP (as presented in the MT3DMS code) was found to be insufficient to reproduce the free convection patterns in the Elder-Voss-Souza problem (Fig. 14a).

The value of NP does not affect the MMOC because only one particle is used to approximate the concentration

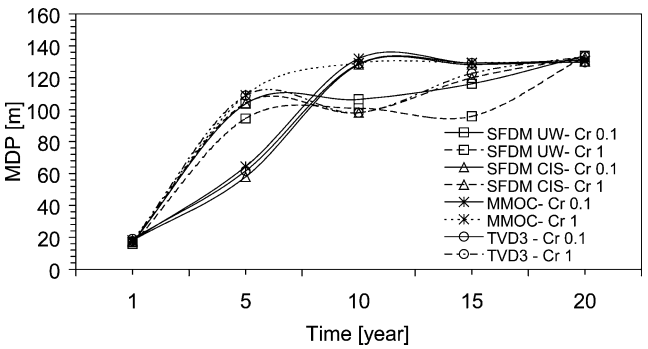

Fig. 12 Maximum depth of penetration (*MDP*) of 0.5 isochlor with time for different *Cr* numbers and numerical schemes

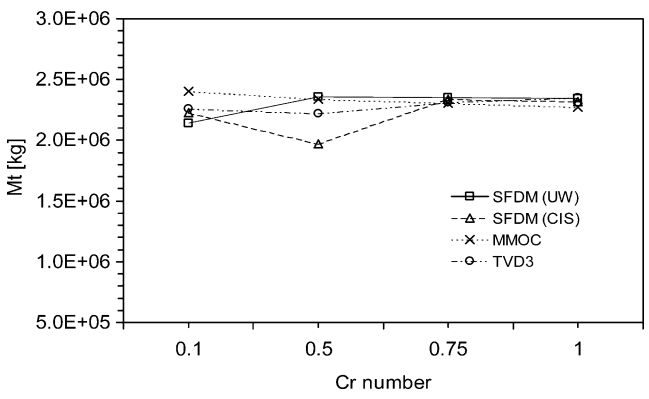

Fig. 13 Total contaminant mass (Mt) in the horizontal slice of 5.5 m thickness the top of which is located at depth 60.5 m below the source, at 10 years for different Cr numbers and numerical schemes

 DOI 10.1007/s10040-007-0164-2

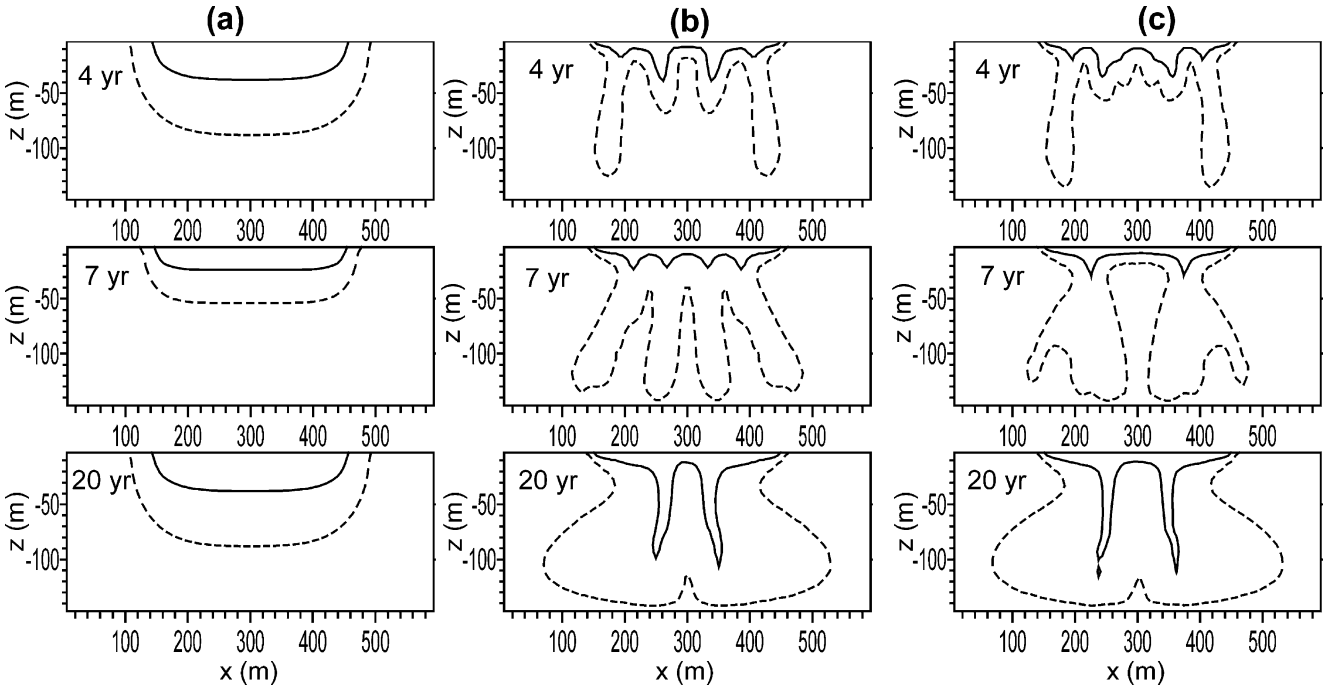

Fig. 14 Contour lines of 0.2 and 0.6 isochlors for MOC at 4, 7, and 20 years. In **a** *MAXPART* is 100,000, *NPPLAN* is 2, *NPL* is 0, *NPH* is 15, *NPMIN* is 0, and *NPMAX* is 15. In **b** *MAXPART* is 100,000, *NPPLAN* is 2, *NPL* is 20, *NPH* is 100, *NPMIN* is 10, and *NPMAX* is 200. In **c** *MAXPART* is 1,000,000, *NPPLAN* is 8, *NPL* is 80, *NPH* is 400, *NPMIN* is 40, and *NPMAX* is 800. See text for explanation

interface between two nodes at each time step. Hence it is more efficient in terms of computational expense compared with MOC and HMOC, but is found to deliver different results (deeper fingers) compared with SFDM (CIS), and TVD3 schemes. The MOC and HMOC were found to produce good results at intermediate mesh size when NP is set high enough. The TVD3 scheme produces good results but is found to be computationally expensive.

Summary and conclusion

This study investigated the sensitivity of the finite difference code SEAWAT to spatial and temporal resolutions as well as solver choice for the unstable Elders-Voss-Souza problem. The major conclusions can be summarized as follows:

1. As expected from previous studies using other codes (e.g., SUTRA and FEFLOW), the spatial resolution level does affect the results in terms of the salinity distribution patterns, the extent and dimensions of fingers, and the total mass at a specified horizontal depth and time. A grid cell size of about 0.38% (dx) and about 0.6% (dz) of the total length and depth of the domain, respectively, is found to be fine enough to produce results with acceptable convergence when Cr is 0.1 for all the selected schemes. Based on both qualitative and quantitative analysis, concentration patterns behave consistently for resolutions equal to or finer than R4 for the various schemes and Cr=0.1.
2. Considering the central up-flow to be the correct pattern, SEAWAT using the MOC or HMOC schemes was able to reproduce this pattern at a coarse mesh (1,188 cells), where other codes like FEFLOW (Kolditz et al. 1998) only do so at finer grids (e.g., 4,539 cells).
3. Temporal discretization was also found to affect the evolving patterns of salinity distribution. At the typical value of Cr (1) and the MT3DMS default value of (Cr=0.75) there were significant differences in the results compared with the case when Cr is 0.1 based on qualitative measures. The quantitative Mt indicator for the different numerical schemes can increase with decreasing Cr. Where most schemes (e.g., MMOC and TVD3) show an insignificant difference in Mt (<2%) over the range of selected Cr numbers, the SFDM schemes are found to be very sensitive to the assigned Cr (16%). Based on the qualitative analysis, in order to minimize the effect of temporal discretization on the concentration results from SEAWAT, Cr should be ≤0.1 when the Pe is ≤1 (R4 and R5).
4. For a given spatial and temporal resolution, the results can vary between the different numerical schemes. For example, the TVD3 scheme produces the (assumed) correct pattern at R3 whereas SFDM (UW) does so only at an extremely fine mesh (R5). Results for most of the

 DOI 10.1007/s10040-007-0164-2

schemes agree qualitatively at high spatial (≥R4) and temporal resolutions (Cr≤0.1).

5. The quantitative measures are generally found to be useful additional indicators for assessing the differences in results. Mt was of limited use in discerning convergence trends between schemes associated with temporal discretization.
6. While the findings of this study may not be directly applicable to other density-dependent problems, they outline an approach for assessing accuracy for SEAWAT users.

Naturally, there are other factors that should be considered along with the spatial and temporal discretizations, like the level of accuracy required, and the computational expense. The computational time in this study varies from 20 min for simulations using R1 to nearly 23 h for R5 a Pentium 4 personal computer with 3 GHz processor and 1 GB RAM.

Acknowledgements The authors would like to acknowledge the support of the Government of Oman and the University of Queensland, Australia.

References

Ackerer Ph, Younes A, Mose R (1999) Modeling variable density flow and solute transport in porous medium: 1. Numerical model and verification. Transp Porous Media 35(3):345–373

Bakker M, Essink G, Langevin CD (2004) The rotating movement of three immiscible fluids: a benchmark problem. Hydrology 287:270–278

Benson DA, Carey AE, Wheatcraft SW (1998) Numerical advective flux in highly variable velocity fields exemplified by saltwater intrusion. Contam Hydrol 34:207–233

Chiang W-H, Kinzelbach W (1998) Processing MODFLOW: a simulation system for modelling groundwater flow and pollution. TU, Hamburg

Diersch H-JG, Kolditz O (1998) Coupled groundwater flow and transport: 2. Thermohaline and 3D convection systems. Adv Water Resour 21(5):401–425

Diersch H-JG, Kolditz O (2002) Variable-density flow and transport in porous media: approaches and challenges. Adv Water Resour 25 (8–12):899–944

Elder J (1967) Transient convection in porous medium. Fluid Mech 27 (3):609–623

Frolkovic P, Schepper HD (2000) Numerical modelling of convection dominated transport coupled with density driven flow in porous media. Adv Water Resour 24:63–72

Guo W, Langevin CD (2002) SEAWAT: a computer program for simulation of three-dimensional variable-density groundwater flow. In: Techniques of water-resources investigations. Book 6, Chapter A7, US Geol Surv, Reston, VA, USA, p 77

Harbaugh AW, Banta ER, Hill MC, McDonald MG (2000) MODFLOW-2000, the U.S. Geological Survey modular ground-water model: user guide to modularization concepts and the groundwater flow process: US Geol Surv Open-File Rep 00–92, p 121

Holzbecher EO (1998) Modeling density-driven flow in porous media, principles, numerics, software. Springer, Berlin Heidelberg New York

Ibaraki M (1998) A robust and efficient numerical model for analysis of density-dependent flow in porous media. Contam Hydrol 34:235–246

Kolditz O, Ratke R, Diersch H-JG, Zielke W (1998) Coupled groundwater flow and transport: 1. verification of variable density flow and transport models. Adv Water Resour 21:27–46

Langevin CD, Guo W (2006) MODFLOW/MT3DMS-based simulation of variable-density groundwater flow and transport. Groundwater 44(3):339–351

Langevin CD, Shoemaker WB, Guo W (2003) MODFLOW-2000, the US Geological Survey modular groundwater model-documentation of the SEAWAT-2000 version with the variable-density flow process (VDF) and the integrated MT3DMS transport process (IMT). US Geol Surv Open-File Rep 03–426, p 43

Mazzia A, Bergamaschi L, Putti M (2001) On the reliability of numerical solution of brine transport in groundwater: analysis of infiltration from a salt lake. Transp Porous Media 43:65–86

McDonald MG, Harbaugh AW (1988) A modular three-dimensional finite-difference ground-water flow model. In: Techniques of water-resources investigations. Book 6, Chap. A1, US Geol Surv, Reston, VA, USA, p 586

Oldenburg CM, Pruess K (1995) Dispersive transport dynamics in a strongly coupled groundwater-brine flow system. Water Resour Res 31:289–302

Oltean C, Bues MA (2001) Coupled groundwater flow and transport in porous media: a conservative or non-conservative form? Transp Porous Media 44:219–246

Prasad A (2000) Density-driven groundwater flow and solute transport in heterogeneous porous media. MSc Thesis, Flinders University, Adelaide, South Australia

Prasad A, Simmons CT (2004) Using quantitative indicators to evaluate results from variable-density groundwater flow models. Hydrology DOI 10.1007/s10040-004-0338-0

Schincariol RA, Schwartz FW (1990) An experimental investigation of variable density flow and mixing in homogeneous and heterogeneous media. Water Resour Res 26(10):2317–2329

Schincariol RA, Schwartz FW, Mendoza CA (1994) On the generation of instabilities in variable density flow. Water Resour Res 30(4):913–927

Schincariol RA, Schwartz FW, Mendoza CA (1997) Instabilities in variable density flows: stability and sensitivity analyses for homogeneous and heterogeneous media. Water Resour Res 33(1):31–41

Simmons CT, Narayan KA (1997) Mixed convection process below a saline disposal basin. Hydrology 194:263–285

Voss CI, Souza WR (1987) Variable density flow and solute transport simulation of regional aquifers containing a narrow freshwater-saltwater transition zone. Water Resour Res 23(10):1851–1866

Weatherill D, Simmons CT, Voss CI, Robinson NI (2004) Testing density-dependent groundwater models: two-dimensional steady state unstable convection in infinite, finite and inclined porous layers. Adv Water Resour 27:547–562

Wooding RA (1969) Growth of fingers at an unstable diffusing interface in a porous medium or Hele-Shaw cell. Fluid Mech 39 (3):447–495

Woods JA, Teubner MD, Simmons CT, Narayan KA (2003) Numerical error in groundwater flow and solute transport simulation. Water Resour Res 39(6):1158

Zhang Q (2000) Seawater intrusion and contaminant transport in costal aquifers. PhD Thesis, The University of Queensland, Australia

Zheng C, Bennett GD (1995) Applied contaminant transport modelling: theory and practice. Reinhold, New York

Zheng C, Wang PP (1999) MT3DMS: a modular three-dimensional multispecies transport model for simulation of advection, dispersion, and chemical reactions of contaminants in groundwater systems: documentation and user's guide. US Army Corps of Engineers, Contract Report SERDP-99-1, University of Alabama, USA

Zimmermann S, Bauer P, Held R, Kinzelbach W, Walther JH (2005) Salt transport on islands in the Okavango Delta: numerical investigations. Adv Water Resour 29(1):11–29